

Effect of Substrate Material on the Microstructure, Texture, Phase and Microhardness of a Ti-48Al-2Cr-2Nb Alloy Processed by Laser Melting Deposition

Liu Zhanqi, Ma Ruixin, Wang Wenbo, Xu Guojian, Su Yunhai

Shenyang University of Technology, Shenyang 110870, China

Abstract: Effect of substrate material on the microstructure, texture, phase and hardness of a Ti-48Al-2Cr-2Nb alloy processed by laser melting deposition (LMD) was investigated. With the increase of the number of deposited layers, the microstructure of the deposited layers changes from basket structure to equiaxed structure and finally evolves into lamellar structure, and $\alpha_2(\text{Ti}_3\text{Al})$ phase decreases and $\gamma(\text{TiAl})$ phase increases gradually. Different TiAl alloy layers show different microhardness. With the increase of the number of deposited layers, the microhardness decreases. The findings will be a valuable reference for fabricating TiAl components with acceptable microstructure, texture, phase compositions and microhardness by LMD.

Key words: laser metal deposition; TiAl alloy; microstructure; phase; microhardness

TiAl alloy has high melting point (above 1450 °C), low density (4 g/cm³), high elastic modulus (160~180 GPa) and high creep strength (up to 900 °C). In recent years, TiAl alloys have gradually replaced titanium alloys, nickel-base superalloys and heat-resistant steels. In the field of aerospace and vehicle engine manufacturing has great potential^[1-3]. When titanium alloy is at higher working temperature, the engine efficiency is higher. Because the strength of titanium alloy will decrease at high temperature for a long time, the high temperature oxidation resistance of titanium alloy is not enough, the working temperature of titanium alloy is usually limited within 500 °C, and the titanium alloy shows poor high temperature oxidation resistance^[4-6]. In addition, their low hardness and poor tribological properties severely restrict their application as key moving parts^[7, 8]. In order to overcome this shortcoming, depositing intermetallic compound coating and ceramic coating on the surface of titanium alloy are an effective method to improve the surface properties of titanium alloy^[9-12]. TiAl alloy is a promising high temperature material and can be used as heat resistant coating. Ti-Al alloys with 40%~50% Al atom

content are called γ -TiAl base alloys^[13]. Commercial γ -TiAl alloys usually contain two phases (γ and α_2) and a small amount of third phase strengthening precipitates^[14].

Among all kinds of materials, TiAl intermetallic compound coating is a promising method to improve the high temperature oxidation resistance and tribological properties of titanium alloys^[15-17]. This is due to the co-existence of metal bonds and covalent bonds in TiAl intermetallic compounds, which provide both the toughness of metals and the high temperature properties of ceramics^[18,19]. In order to improve the wear resistance of titanium alloys, many researchers prepared various TiAl intermetallic compound composite coatings by laser surface treatment. For example, Li et al^[20] reported the Al coating was prepared by laser cladding Ti6Al4V alloy with the mixture of pure Ti₃Al/TiAl powder. The results show that the wear resistance of the Ti₃Al/TiAl coating is about 2 times of that of the original TC4 substrate. The appearance of cracks in the coatings often lead to the serious degradation of the coating properties^[21-23]. For example, Li et al^[20] observed that cracks appeared on the surface of Ti₃Al/TiAl ceramic layer, and the

Received date: July 12, 2019

Foundation item: Intelligent Additive Manufacturing System Platform (2017YFB1103600)

Corresponding author: Xu Guojian, Ph. D., Professor, School of Materials Science and Engineering, Shenyang University of Technology, Shenyang 110870, P. R. China, E-mail: xuguojian1959@qq.com

Copyright © 2020, Northwest Institute for Nonferrous Metal Research. Published by Science Press. All rights reserved.

ceramic layer partly fell off during the wear process, which resulted in the decrease of wear resistance of the coating. It is considered that the crack is caused by the fact that the thermal stress is greater than the limit of the yield strength of the ceramic layer.

Laser cladding is an advanced technology to improve the wear and oxidation properties of titanium alloys. Compared with chemical vapor deposition (CVD), physical vapor deposition (PVD) and thermal spraying, laser deposition manufacturing (LDM) has the advantages of short processing time, flexible operation and high precision^[24-27]. It has been widely used in the surface modification of metals and alloys. LDM technology has the advantages of high density, good metallurgical bond between coating and substrate, controllable coating thickness, high efficiency, high flexibility and so on.

LDM has broad application prospects in the preparation of TiAl intermetallic compound sample. However, there are few reports on the preparation of γ -TiAl alloy by LDM technology, and systematic research results are urgently needed. Therefore, this work concentrates on investigating the influence of substrate material on the microstructure, crystallographic texture, phase transition and microhardness of a Ti-48Al-2Cr-2Nb alloy processed by LDM.

1 Experiment

The powder material is Ti-48Al-2Cr-2Nb alloy (the particle size is 53 μm ~150 μm), and chemical composition of Ti-48Al-2Cr-2Nb alloy powder is Al 32.5 wt%, Cr 2.64 wt%, Nb 4.62 wt%, O 0.06 wt%, N 0.005 wt%, Ti Bal. The alloy powder was dried at 150 °C for 1.5 h. The substrate material was TC4 titanium alloy. The size of the substrate was 100 mm \times 100 mm \times 20 mm. Oxide film and oil stains on the substrate surface were removed by a grinding machine and acetone. The printing equipment was LDM8060 produced by Nanjing Zhongke Yuchen Laser Technology Co., Ltd of China. Semiconductor laser LDF4000-100 was produced by Shenzhen Keyi Instrument Co., Ltd of China. During the test, the diameter of laser focal spot was 3 mm, the defocus is 0 mm, argon gas flow rate of powder feeding gas was 8 L/min, the preheating temperature of substrate was 350 °C. The protective gas in the sealed work box is 99.99% argon gas, and the content of water and oxygen in the sealed work box is $\leq 50 \mu\text{L/L}$.

The deposited samples were cut into 10 mm \times 10 mm \times 10 mm blocks by wire-cutting machine for microstructure analysis. Then the blocks were ground with sandpaper (sandpaper type was 800#, 100#, 150#, 200#), and then polished with ET-500 environment-friendly spray polishing agent (particle size is 2.5, 1.5, 0.5 μm). The corrosion solution is Kroll solution (volume ratio is HF:HNO₃:H₂O=2:3:10) and the corrosion time was about 15 s. After corrosion, the corrosion solution was washed with alcohol and

dried with air tube. The microstructure and composition of the deposited layers were analyzed by Hitachi SU8010N field emission scanning electron microscope (SEM). The deposited layers were analyzed by EBSD with Gemini SEM300 model, and the phase composition of deposited layers was analyzed by X-7000 X-ray diffractometer. The Vickers hardness distribution was measured by HVS-5 Vickers hardness tester (load is 200 g, duration is 10 s).

2 Results and Discussion

2.1 Appearance of the deposited sample

Fig.1 shows the appearance of the deposited layers. The technological parameters of LDM are as follows: laser power 1400 W, scanning speed 7 mm/s, powder feeding speed 5.67 g/min (0.8 r/min), lap ratio 50%, layer thickness 0.4 mm. The length and width size of the deposited layers is 40 mm \times 40 mm. During printing, the laser path is shown in Fig.1a. Five layers of TiAl alloy were deposited on TC4 titanium alloy substrate, and the results are shown in Fig.1b. The cross print route can reduce the stress value, which can reduce the formation of cracks.

2.2 Microstructure of deposited sample

Fig.2 shows SEM images of different deposited layers. Fig.2a~2f shows the morphologies from substrate to the fifth layers. It can be seen from Fig.2 that the microstructure of the first layer of TiAl alloy is net basket structure. The microstructure of the second layer TiAl alloy is needle-like structure. From the microstructure of the third layer TiAl alloy, it can be seen that the needle-like structure is partly formed into block structure. From the microstructure of the fourth layer TiAl alloy, it can be seen that the needle-like structure is all transformed into bulk structure. From the microstructure of the fifth layer TiAl alloy, it can be seen that most of the bulk microstructure is transformed into lamellar structure. As can be seen from Fig.2, the microstructure of TC4 alloy is basket structure, and γ -TiAl is lamellar structure. During the laser melting deposition of γ -TiAl alloy, the transition of transition layer will occur between the substrate and the γ -TiAl alloy due to the dilution of the substrate TC4 alloy. From the experimental results, it can be seen that the transition process is from the

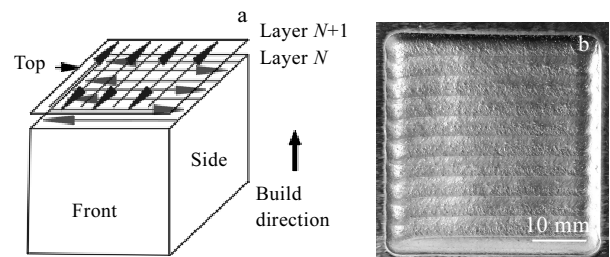


Fig.1 Schematic (a) and physical image (b) of deposited layers

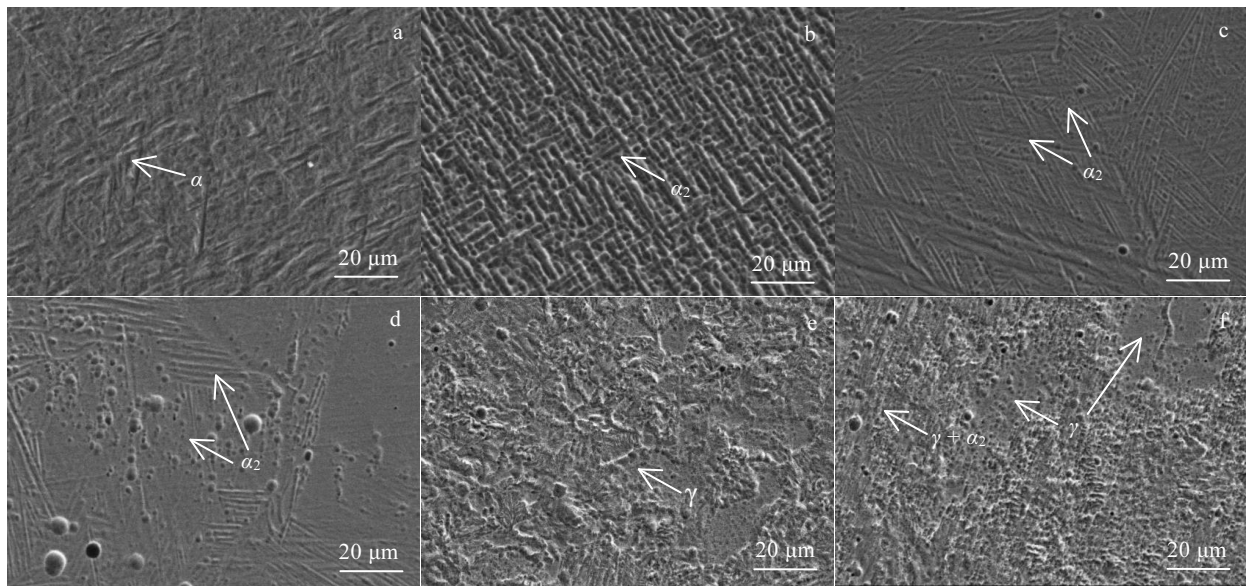


Fig.2 SEM image of deposited layers: (a) substrate, (b) the first layer, (c) the second layer, (d) the third layer, (e) the fourth layer, and (f) the fifth layer

basket to the isometric last to the lamellar transition process. The transformation process is mainly controlled by the content of Al elements.

2.3 Phase structure and element distribution of deposited layers

Fig.3 is the XRD patterns of substrate and deposited layers. It can be seen that the TC4 substrate is mainly composed of α phase, and the first layer is mainly composed of α_2 phase. The phase composition of the third layers and first layer does not change obviously. The phase composition of the fifth layers is mainly γ phase and a small amount of α_2 . The effect of TC4 titanium alloy substrate on the deposited layers can be seen from the analysis results of surface scan in Fig.4.

The crystal structure of α_2 phase is DO19 type, which is an ordered hexagonal α phase. The α_2 phase is characterized by high hardness and poor plasticity.

From the EDS results in Fig.4b, 4c, it is evident that with the increase of the number of deposited layers, the content of Al element increases gradually, while the contents of Ti element gradually decreases, due to the most prominent changes in the contents of Al and Ti elements in the first three layers. The results show that the substrate material has a great influence on the first three layers of the deposited samples.

2.4 Crystal orientation, phase distribution and texture direction of the deposited layers

The orientation scale is shown in Fig.5a, representing the relationship between colors in the EBSD images

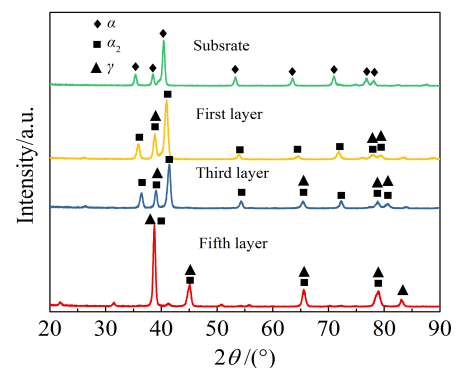


Fig.3 XRD patterns of substrate and deposited layers

and crystal orientations of the LMD-processed sample^[28]. The EBSD orientation image map of the sample first, third and fifth layers from the top view are illustrated in Fig.5b, 5c and 5d, respectively. The applied substrate material significantly influences the crystal morphology and orientation of the LMD-processed Ti-48Al-2Cr-2Nb alloy. In the first layer, the majority of the crystal have a purple-red color as shown in Fig.5b. The crystal at $(01\bar{1}0)$ and (0001) orientations are present. The morphology of the crystal is the structure of the net basket. In the third layer, the majority of the crystal have a green-blue color as shown in Fig.5c. The crystal at $(01\bar{1}0)$ and $(\bar{1}2\bar{1}0)$ orientations are present. It can be easily found that the blue areas increase

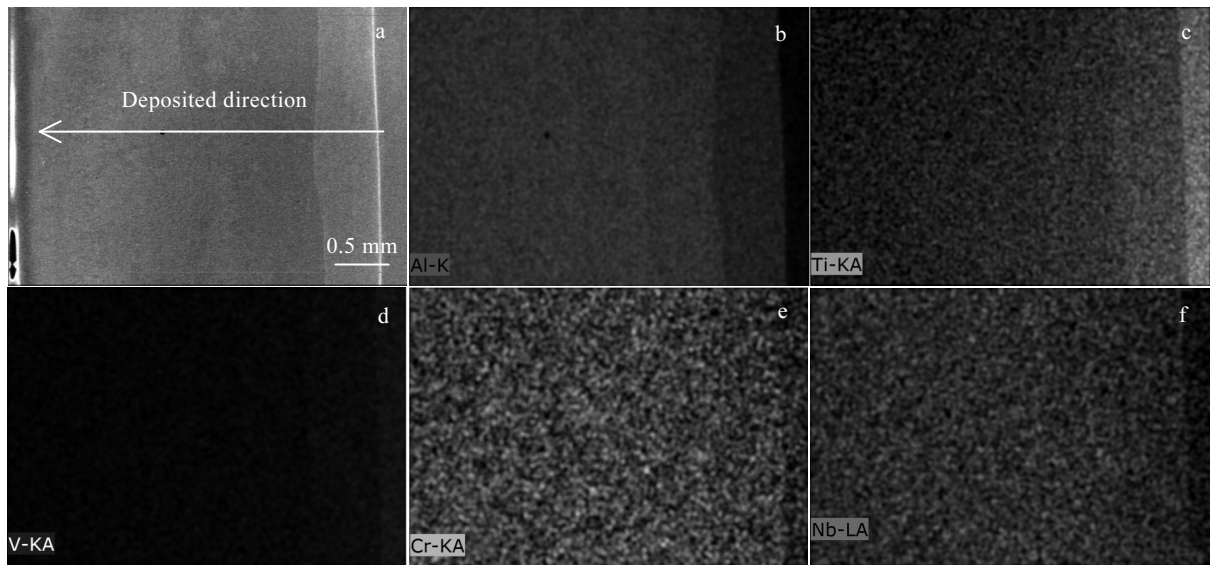


Fig.4 SEM image (a) and EDS element line scanning (b~f) of deposited layers: (b) Al, (c) Ti, (d) V, (e) Cr, and (f) Nb

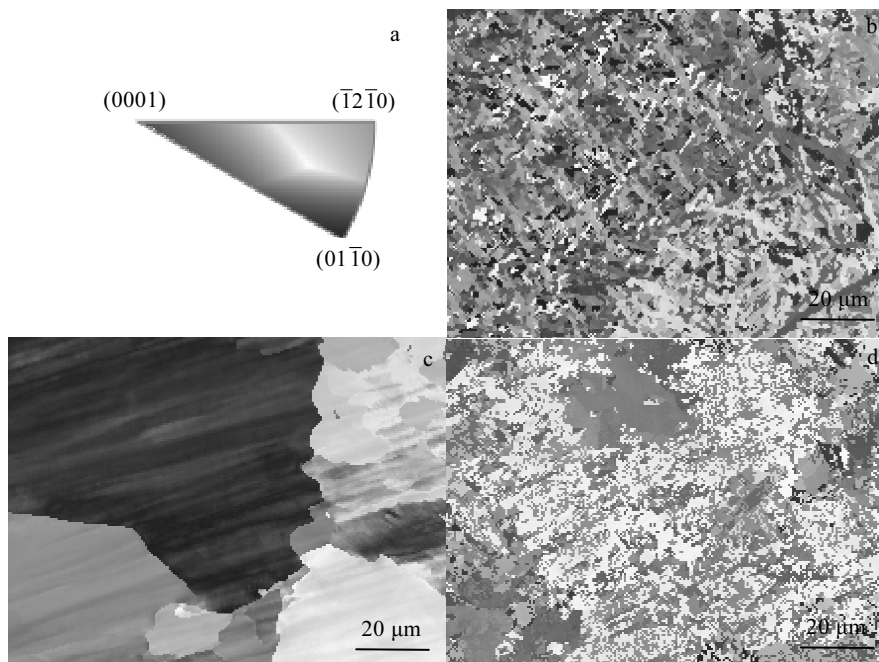


Fig.5 Crystal orientation of deposited layers at the top view: (a) orientation scale, (b) first-layer orientation map, (c) third-layer orientation map, and (d) fifth-layer orientation map

while the purple regions decrease in the EBSD map in Fig.5c compared with that in Fig.5b, indicating that the $(01\bar{1}0)$ orientation is strengthened on the top view of sample. The morphology of the crystal is the structure of the block. In the fifth layer, the majority of the crystal have a blue-white color as shown in Fig.5d. It can be easily found that the white areas increase while the blue regions

decrease in the EBSD map in Fig.5d compared with that in Fig.5c. The morphology of the crystal is the structure of the lamellar. Because the structure of the first layer is most seriously affected by the substrate material, the morphology of the structure is a net basket structure. From the microstructure of the fifth layer, it can be seen that the influence of substrate material on the deposited layer ba-

sically disappears. Therefore, the substrate material not only has an effect on the microstructure, but also has an effect on the crystal orientation.

Fig.6 shows the distribution of SEM images of the first, third and fifth layers. The blue area represents the α_2 phase and the red region represents the γ phase. It can be seen from the phase figures that almost all the structures of the first and third layers are composed of α_2 phase. The percentage of α_2 phase and γ phase in the fifth layers is 10.7% and 89.3%, respectively. The results show that the effect of TC4 titanium alloy substrate on the deposited layers is mainly concentrated in the front of the fifth layers.

Fig.7 is a polar figures of the first, third, fifth layers. With

the increase of the number of deposited layers, the orientation of crystal texture of α_2 phase is enhanced. The polar figures in Fig.7c and 7d show that the distribution of the crystal texture directions of α_2 and γ phases in the fifth layers is approximately center-symmetric.

2.5 Hardness distribution of deposited layers

The Vickers hardness test results of the deposited layers are shown in Fig.8a and 8b. Fig.8a shows the transverse hardness distribution of TC4 substrate, first, third and fifth layers. It can be seen from the results of hardness test that the hardness of TC4 substrate is the lowest. In addition, with the increase of the number of deposited layers, the hardness value decreases. The average hardness ($HV_{0.2}$) of TC4 sub-

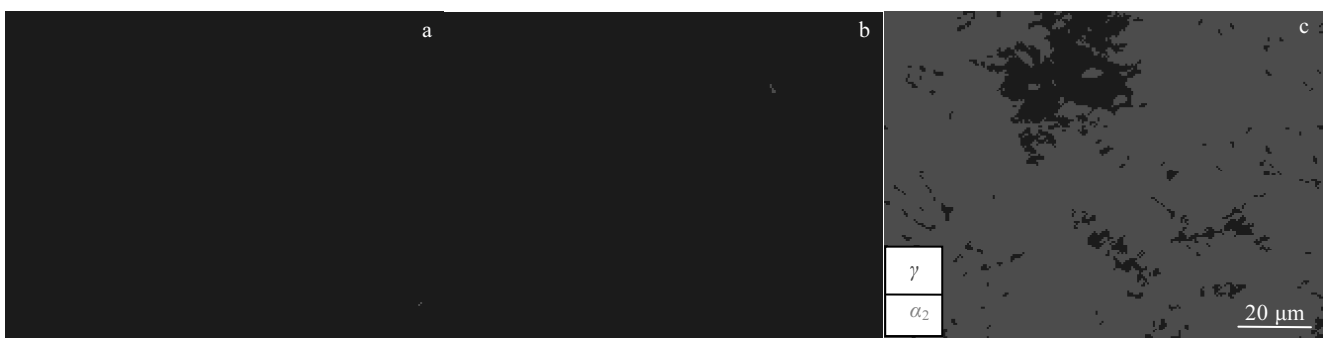


Fig.6 SEM images of deposited layers in the top view: (a) the first layer, (b) the third layer, and (c) the fifth layer

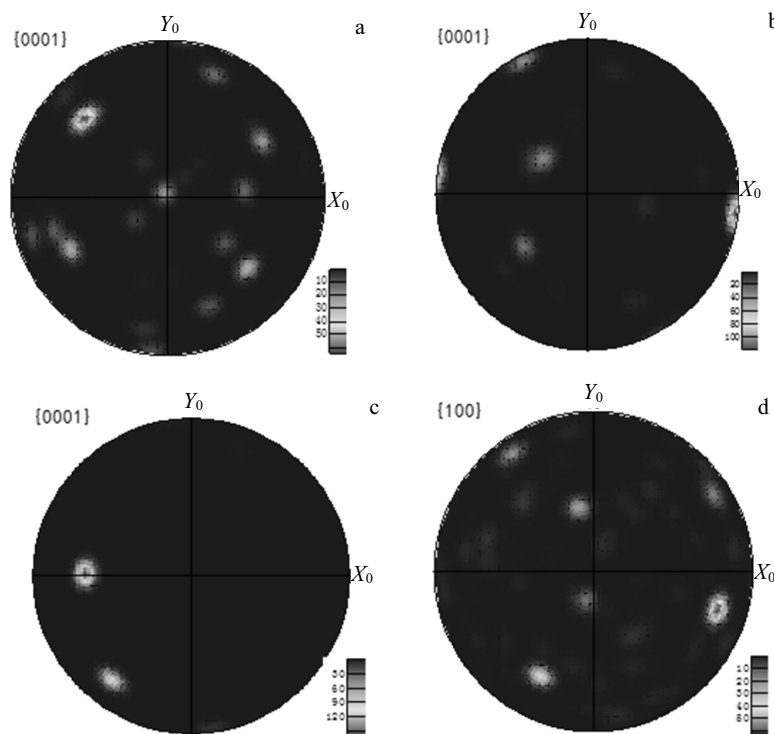


Fig.7 Polar figures of deposited layers in the top view: (a) α_2 phase of the first layer, (b) α_2 phase of the third layer, (c) α_2 phase of the fifth layer, and (d) γ phase of the fifth layer

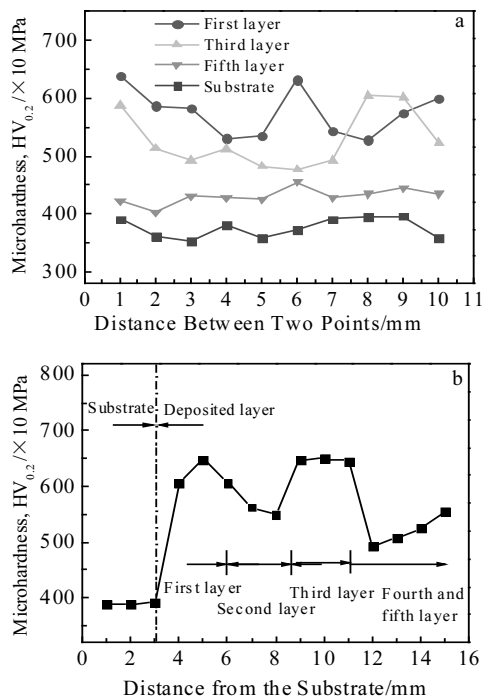


Fig.8 Hardness distribution of deposited layers: (a)transverse distribution and (b) longitudinal distribution

substrate is 3760 MPa, and the average hardness ($HV_{0.2}$) of the first, third and fifth layers is 5750, 5280 and 4310 MPa, respectively. There are several main reasons for the different hardness of the deposited layers, one of which is that the microstructure of first and third layers is composed of α_2 phase, but the microstructure of first layer is finer grains than that of the third layers. The microstructure of the five layers is composed of α_2 and γ phases, and the hardness value of γ phase is lower than that of α_2 phase, so the hardness value of five layers is the smallest.

The second reason is that the maximum residual stress of the deposited sample is mainly distributed in the bottom of the sample and in the middle of the sample, and there is a trend of decreasing from the substrate to the top layer, which can be inferred from the conclusion in the references^[29].

The third reason is that the microhardness value of the same deposited layer increases with the increase of cooling rate within a certain range, because the layer spacing decreases with the increase of cooling rate. Thus, the hardness value of the deposited layer is affected, which can be inferred from the references^[30].

Fig.8b shows the results of the longitudinal hardness distribution of the deposited layers. It can be found that the hardness distribution of the deposited layers is consistent with the transverse hardness distribution.

3 Conclusions

1) Crystal microstructure, orientations, texture, phase composition and microhardness can be tailored by controlling the dilution rate of substrate materials during LDM. Because the deposited layers are diluted by the substrate material, the α_2 phase in the deposited layers increases, α_2 phase belongs to the dense hexagonal structure, the brittleness is large, and it is sensitive to cracks, so it is of great significance to reduce the dilution rate for the manufacture of TiAl alloy.

2) The hardness distribution characteristics of the deposited layers are mainly related to the α_2 phase content. The higher the content of α_2 phase in the deposited layers, the higher the microhardness value. The microhardness value may also be affected by the residual stress and cooling rate.

3) The findings would be a valuable reference to the optimization of the dilution rate for fabricating TiAl components with acceptable crystal microstructure, phase compositions and microhardness by LDM.

References

- 1 Qu H P, Li P, Zhang S Q et al. *Materials & Design*[J], 2010, 31(4): 2201
- 2 Biamino S, Penna A, Ackelid U et al. *Intermetallics*[J], 2011, 19: 776
- 3 Yang Guangyu, Jia Wenpeng, Zhao Pei et al. *Rare Metal Materials and Engineering*[J], 2016, 45 (7): 1683
- 4 Dai Jingjie, Li Shouying, Zhang Hongxia et al. *Surface & Coatings Technology*[J], 2018, 344(25): 479
- 5 Liu Fencheng, Mao Yuqing, Lin Xin et al. *Optics & Laser Technology*[J], 2016, 83: 140
- 6 Niu Ruili, Li Jinlong, Wang Yongxin et al. *Surface and Coatings Technology*[J], 2017, 309(15): 232
- 7 Huang Can, Zhang Yongzhong, Vilar Rui et al. *Materials & Design*[J], 2012, 41: 338
- 8 Fu Yao, Zhang Xiancheng, Sui Jianfeng et al. *Optics & Laser Technology*[J], 2015, 67: 78
- 9 Tlotleng M, Masina B, Pityana S. *Procedia Manufacturing*[J], 2017, 7: 39
- 10 Han Peng, Kou Hongchao, Yang Jieren et al. *Rare Metals*[J], 2016, 35 (1): 35
- 11 Chen Guoqing, Zhang Binggang, Liu Wei et al. *Rare Metal Materials and Engineering*[J], 2013, 42(3): 452
- 12 Xue Z, Yang Q, Gu L et al. *Materialwissenschaft Und Werkstofftechnik*[J], 2015, 46(1): 40
- 13 Hao Yanjun, Liu Jinxu, Li Jianchong et al. *Rare Metal Materials and Engineering*[J], 2017, 46(3): 754
- 14 Liu Yi, Hu Rui, Kou Hongchao et al. *Materials Characterization*[J], 2015, 100: 104
- 15 Wu Liankui, Xia Junjie, Cao Huazhen et al. *Oxidation of Metals*[J], 2018, 90(5-6): 617
- 16 Nie Ge, Ding Hongsheng, Chen Ruirun et al. *Materials & Design*[J], 2012, 39: 350
- 17 Bao Panfei, Song Xiaoguo, Wang Xinbo et al. *Rare Metal*

- Materials and Engineering*[J], 2018, 47(7): 2132
- 18 Du Y J, Rao K P, Chung J C Y et al. *Metallurgical and Materials Transactions A*[J], 2000, 31(3): 763
- 19 Gizynski M, Miyazaki S, Sienkiewicz J et al. *Surface and Coatings Technology*[J], 2017, 315(15): 240
- 20 Li Jianing, Chen Chuanzhong, Squartini Tiziano et al. *Applied Surface Science*[J], 2010, 257(5): 1550
- 21 Espejo H M, Bahr D F. *Surface and Coatings Technology*[J], 2017, 322(15): 46
- 22 Gussone Joachim, Hagedorn Yves-Christian, Gherekhloo Human et al. *Intermetallics*[J], 2015, 66: 133
- 23 Guo Chun, Zhou Jiansong, Chen Jianmin et al. *Surface and Coatings Technology*[J], 2010, 205(7): 2142
- 24 Kunal K, Ramachandran R, Norman M W. *Progress in Aerospace Sciences*[J], 2012, 55: 1
- 25 Maliutina L N, Si-Mohand H, Sijobert J. *Surface and Coatings Technology*[J], 2017, 319(15): 136
- 26 Liu Hongxi, Zhang Xiaowei, Jiang Yehua et al. *Journal of Alloys Compounds*[J], 2016, 670(15): 268
- 27 Zhai Yongjie, Liu Xiubo, Qiao Shijie et al. *Optics & Laser Technology*[J], 2017, 89: 97
- 28 Li Wei, Liu Jie, Zhou Yan et al. *Scripta Materialia*[J], 2016, 118: 13
- 29 Wang Junfei, Yuan Juntang, Wang Zhenhua et al. *Laser Technology*[J], 2019, 43(3): 41 (in Chinese)
- 30 Fei Yue, Wang Xinnan, Shang Guoqiang et al. *Chinese Journal of Rare Metals*[J], 2017, 41(9): 1056 (in Chinese)

基板材料对激光熔化沉积制造 Ti-48Al-2Cr-2Nb 合金组织、织构、相和显微硬度的影响

刘占起, 马瑞鑫, 王文博, 徐国建, 苏允海

(沈阳工业大学, 辽宁 沈阳 110870)

摘要: 研究了基体材料对激光熔化沉积 Ti-48Al-2Cr-2Nb 合金显微组织、织构、相组成和硬度的影响。随着沉积层数的增加, 沉积层的显微组织由网篮状结构向等轴状结构转变, 最终演变为层状结构。 $\alpha_2(\text{Ti}_3\text{Al})$ 相逐渐减少, $\gamma(\text{TiAl})$ 相逐渐增多。不同的 TiAl 合金层具有不同的显微硬度, 随着沉积层数的增加, 显微硬度降低。研究结果对于激光沉积制造 TiAl 合金制备具有可接受的组织、织构、相组成和显微硬度具有参考价值。

关键词: 激光熔化沉积; TiAl合金; 显微组织; 相; 显微硬度

作者简介: 刘占起, 男, 1990年生, 博士, 沈阳工业大学材料科学与工程学院, 辽宁 沈阳 110870, E-mail: 1640754283@qq.com